Evaluating tephrochronology in the permafrost peatlands of Northern Sweden

Claire L. Cooper*[1,2], Graeme T. Swindles[1,3], Elizabeth J. Watson[1], Ivan P. Savov[2], Mariusz Galka[4], Angela Gallego-Sala[5], Werner Borken[6]

[1] School of Geography, University of Leeds, UK, LS2 9JT

[2] School of Earth and Environment, University of Leeds, UK, LS2 9JT

[3] Ottawa-Carleton Geoscience Centre and Department of Earth Sciences, Carleton University, Canada

[4] Dept. of Biogeography and Palaeoecology, Adam Mickiewicz University, Poland

[5] School of Geography, University of Exeter, UK, EX4 4RJ

[6] Dept. of Soil Ecology, University of Bayreuth, Germany

* Corresponding author: *gyclc@leeds.ac.uk*

For submission to: *Quaternary Geochronology*

Keywords: *tephra; peatlands; permafrost; glass preservation; tephrochronology*

Highlights

- Six tephra layers are identified in sub-Arctic peatlands at Abisko, Sweden
- Geochemical analyses of glass shards are presented, identifying material belonging to the Hekla 4, Hekla-Selsund, Hekla 1104, and Hekla 1158 eruptions
- Variation in the deposition and preservation of tephra layers across adjacent profiles is identified and discussed

Abstract

Tephrochronology is an increasingly important tool for the dating of sediment and peat profiles for palaeoecological, palaeoclimatic and archaeological research. However, although much work has been done on tephra in temperate peatlands, there have been very few in-depth investigations of permafrost peatlands. Here we present the analysis of nine peatland cores from Abisko, northern Sweden, and show that the presence of tephra layers may be highly variable even over a scale of <10 km. Using electron probe microanalysis (EPMA) combined with age-depth profiles compiled from radiocarbon (^{14}C) and ^{210}Pb dating of peat records, we identify the Hekla 1104, Hekla 1158, Hekla-Selsund and the Hekla 4 tephra layers. We also infer the presence of the Askja 1875 tephra, in addition to an unassigned tephra dating from between 1971-1987 AD in two separate cores. Five of the nine analysed cores do not contain distinct tephra layers. Volcanic ash deposits in northern Scandinavia are subject to both regional-scale variations in climate and atmospheric circulation, and local-scale variations on the order of tens of kilometres in topography, vegetation, snow cover, and ground permeability. The extreme inconsistency of

tephra preservation within a small study area (~3000 km^2) brings into question the reliability of tephrochronology within permafrost peatlands, and highlights the necessity of alternative methods for dating peat profiles in this region.

1 Introduction

The study of volcanic ash preserved in peatlands and lake sediments is a well-established science, particularly across western Europe and North America (Lowe, 2011; Stivrins et al., 2016; Watson et al., 2016a; Plunkett et al., 2018; Swindles et al., 2018). Light ash particles from volcanic eruptions are carried across continents by atmospheric currents, sometimes being transported thousands of kilometres from their source (Cadle et al., 1976; Palais et al., 1992; Bourne et al., 2016). The fallout from these eruptions may then be preserved in layers in soft sediments such as in peatlands and lakes, providing useful markers and isochrons across multiple sites. Tephra layers linked to particular eruptions allow sediment profiles to be correlated to specific points in time. Assuming that ash deposition occurs approximately simultaneously across multiple sites, applying tephrochronology to a given record allows for precise, high-resolution chronological reconstruction of sediment columns, with a range of environmental and archaeological applications (Lowe et al., 2011; Lane et al., 2014). However, relatively few tephrochronological studies have been performed on permafrost peatlands in Europe compared to temperate peatlands (Watson et al., 2016).

Abisko Scientific Research Station is located in the Scandinavian Arctic, approximately 30 kilometres north of the polar circle at 68°21’ N, 18°49’E. The station has a long history of wide-ranging environmental and ecological research, with many recent studies focusing on the observations and effects of climate change in a boreal environment (Alatalo et al., 2016; Lundin et al., 2016; Lett, 2017). Rapid alterations in the local climate over the past 50 years and an increase in the frequency of winter warming events in northern Scandinavia (Vikhamar-Schuler et al., 2016) have caused significant ecological concern. The warmer conditions have been linked to vast reductions in the extent of permafrost in the area (Osterkamp & Romanovsky, 1999; Camill, 2003; Schuur & Abbott, 2011), affecting the surface water pH, water table depth and vegetation in permafrost peatlands (Camill, 1999).

Wetlands have long been acknowledged as playing a significant role in global carbon emissions and sequestration (Lai, 2009). It is therefore increasingly important for the scientific community to develop an understanding of how permafrost peatlands in this area have changed over time in terms of their ecology, hydrology and carbon accumulation (Swindles et al., 2015b). Accurate and precise chronological control is a crucial component of such investigations into peat archives.

Projections of jet stream currents in the northern hemisphere suggest that, under typical atmospheric circulation conditions, ash particles injected into the stratosphere by Icelandic eruptions should be carried and deposited across much of north-western Europe, including Scandinavia (Woollings et al., 2010; Davies et al., 2010). Past studies have borne this assumption out, and Icelandic tephra has been found across the UK, Ireland, France, Germany, Poland, Belgium, Switzerland, Denmark, Sweden, Norway, and the Faroe Islands (Swindles et al., 2011; Lowe et al., 2011; Watson et al., 2017). However, some disparity between the sediment records of adjacent sites has been noted at several locations (Watson et al., 2016b). Vegetation, local weather at the time of deposition, pH conditions in the sediment, and storm events can all affect the capture and preservation of glass shards (Watson et al., 2016a), resulting in variation across cores, even over distances of a few kilometres. Northern Scandinavia is on the extreme distal edge of most numerical simulations reconstructing Icelandic ash clouds (Davies et al., 2010), making consistent ash fall across wide areas possible, but unlikely. In this paper, we investigate the cryptotephra content (distal tephra <150 µm along the longest axis) of nine cores collected in the vicinity of the Abisko field station. We also discuss the factors affecting shard preservation variability in the area, and consider the implications for future tephrochronological research in this region.

2 Materials and Methods

2.1 Study Area

[Figure 1: Map of study area, showing local topography and the location of coring sites]

Nine samples were collected from peatland sites near Abisko, northern Sweden, seen in Figure 1, using a Russian peat corer. Each sample is between 20-45 cm in depth, and is comprised largely of peat, in addition to occasional lenses of organic mud.

Abisko is located within the rain shadow of the Norwegian mountains, and as such receives a relatively small amount of precipitation (332 mm per year; Callaghan et al., 2010), with the highest rainfall occurring during the summer months. Each of the peatlands sampled were part of peat complexes in various stages of permafrost decomposition, from early dome collapse to full inundation after permafrost thaw. The peatlands of the region are primarily composed of ombotrophic bogs, peat plateaus, arctic fens, and palsa mires, many of which are in states of permafrost collapse as a result of rapid warming. Recent studies have shown an increased rate of permafrost decay in some of the Abisko sites, such as Stordalen (Swindles et al., 2015b)

2.2 Methods

Coring locations were selected on the basis of physical features, hydrology, and vegetation composition (Swindles et al., 2015a). Sites were deemed suitable if they were situated on relatively flat ground, and could be characterised as fens, bogs, or palsas. Full site details may be found in appendix C. The cores were stored in plastic wrap and aluminium foil, and kept at a temperature of 4˚C prior to analysis. Extraction of the tephra in these sediment samples was performed following the method detailed by De Vleeschouwer et al., 2010. Each peat core was divided into continuous sections of 1cm depth, and a sample of 4 cm^3 was removed from each. These samples were weighed and dried in ceramic crucibles at 105^{o}C for a minimum of 12 hours. The dry samples were then reduced to ashes in a muffle furnace at 600^{o}C for six hours. After each stage of burning and drying, the samples were weighed to estimate gravimetric water content and mass loss on ignition. These ashes were suspended in 10% hydrochloric acid for 24 hours to remove carbonate material, and then washed with deionised water. The tephra was concentrated at the bottom of the test tubes by placing the aqueous samples in a centrifuge at 3000 r.p.m. for approximately five minutes. This aqueous material was then sieved through a 10μm mesh. Petrographic slides were prepared by adding the aqueous solution to a glass slide on a hotplate until the liquid component evaporated. The slides were mounted using Histomount and a glass coverslip, and examined through optical microscopy using 200-400x magnification to assess tephra content. References to several visual and descriptive sources were used to ensure positive tephra identification (Lowe, 2011; Watson et al., 2016a).

Sub-samples which were found to contain more than 10 shards per cm^3 were re-sampled and processed using the acid digestion method outlined in Dugmore & Newton (1992), and, later, to density separation, to fully remove problematic organic material and biogenic silica (Blockley et al., 2005). In some cases, tephra was found to exist in irregular, non-continuous, discrete clumps of material rather than in well-defined layers, making repeated extractions from a particular depth within the peat profile problematic. In these instances, optical slides containing tephra were submerged in a xylene solution for 48 hours to dissolve the mounting agent (Ravikumar et al., 2014). This method was found to be highly effective in retaining the tephra and organic material while completely removing the Histomount. Samples for geochemical analysis were then dried, remounted in blocks of resin and subjected to electron probe microanalysis EPMA at the Tephra Analytical Unit, University of Edinburgh. All analysis was performed using a 5μm diameter beam of 15kV with a current of either 2nA (Na, Mg, Al, Si, K, Ca, and Fe) or 80nA (P, Ti, Mn), following the method of Hayward (2012). Lipari and BCR-2G basalt glass standards were used for external calibration (Watson et al., 2015). The standard data generated during geochemical analysis may be found in table B.2 in the appendices. The overall data for the standards returns <1% variability for most major elements.

Radiocarbon signatures of organic material were determined by accelerator mass spectrometry (AMS). Subsamples of 0.8 mg C were combusted in 6 mm sealed quartz tubes with 60 mg CuO oxidizer and 1 cm silver wire for 2 hours at 900°C. The resulting CO_2 was purified from water and non-condensable compounds. Afterwards, CO_2 was reduced to graphite using the zinc reduction method where TiH_2 and Zn with Fe act as catalysts at 550°C for 7.5 hours (Xu et al., 2007). All preparations took place at the Department of Soil Ecology at the University of Bayreuth. The graphite targets were analysed by the Keck-CCAMS facility of the University of California, Irvine, with a precision of 2–3‰ (‰ deviation is from the $^{14}C/^{12}C$ ratio of oxalic acid standard in 1950). The samples were corrected to a $\delta^{13}C$ value of -25‰ to account for any mass dependent fractionation effects (Stuiver & Polach, 1977). Radiocarbon signatures were converted to ^{14}C age before present (BP) using the IntCal13 calibration curve (Reimer et al., 2013). Full radiocarbon dating results may be found in table A.1 in the appendices.

Further chronological data for the Marooned and Stordalen cores was established through ^{210}Pb dating. Peat samples were digested using a combination of concentrated HCl, HNO_3, and H_2O_2. A small amount of ^{209}Po was then added as a tracer. Following the method detailed in Whittle & Gallego-Sala (2016), the material was plated onto silver disks, and alpha spectrometry was performed using an Ortec

Octête Plus Integrated Alpha-Spectrometry System at the University of Exeter (UK) Radiometry Lab. ^{210}Pb values were derived from the $^{210}Po/^{209}Po$ ratios, and dates were then extrapolated from the ^{210}Pb inventory using the constant rate of supply model (Appleby, 2001).

3 Results

3.1 Tephrostratigraphies

[Figure 2: Tephrostratigraphic profiles of Abisko peat cores. Radiocarbon dates (cal BP) are shown in red along the vertical axes. a) Crater Pool 1; b) Crater Pool 2; c) Eagle Bog; d) Electric Bog; e) Instrument Core; f) Nikka Bog; g) Marooned Bog; h) Railway Bog; i) Stordalen Core]

Figure 2 shows the tephra counts per 4 cm^3 of the eight peat profiles collected in Abisko, along with the percentage loss on ignition, and age-depth models based on radiocarbon dating of organic material. While four profiles – Stordalen (ST), Marooned (MN), Eagle (EA), and Nikka (NI) – have clear tephra peaks at varying depths, the other profiles have only minimal volcanic ash content, averaging only 1-3 glass shards per section. There is little to no consistency in the presence of tephra with depth across the profiles. The loss-on-ignition for each profile is high, typically between 80 – 90 %, but there is no apparent correlation with the presence of glass. The glass shards themselves were typically between 10-150 µm, though a wide range of morphologies were present, from thin, concave, wisp-like structures to larger aggregate shards. As the shards in EA12 and NI8 were found to be too small and sparse to perform EPMA, ^{210}Pb dating of the profiles containing these layers was used to determine their ages. The major element geochemistry of the glass found in the Marooned and Stordalen cores can be found in figure 4. Full geochemistries and profile dates may be found in the appendices.

[Figure 3: Age-depth models of Eagle, Nikka, and Stordalen peatland profiles. Tephra profiles identified in this paper are marked in red. Full radiocarbon and ^{210}Pb data can be found in appendix A.]

3.1.1 MN85/Hekla 4

Figure 4 shows the geochemistry of tephra shards found at in the Marooned and Stordalen cores. Shards matching the geochemistry of the Hekla 4 eruption were found at a depth of 85 cm in the Marooned bog core. The Hekla 4 eruption represents the most widespread tephra deposit in northern Europe, and relates to a plinian eruption of Hekla occurring between 2395-2297 BC (Pilcher & Hall, 1996; Watson et al., 2017). Tephra attributed to this deposit occurs across a range of compositions from dacitic to rhyolitic; in the case of the tephra found in Marooned bog, the silica content ranges between 63 – 77 %.

3.1.2 MN70/Hekla-Selsund

The Hekla-Selsund tephra, also known as the Kebister tephra, is dated as occurring between 1800-1750 BC, and can be found in multiple sites across north-western Europe, including Germany, Great Britain, the Faroe Islands and Scandinavia (Watson et al., 2017). In Abisko, it occurs in the Marooned bog core at a depth of 70 cm. This tephra is rhyolitic to dacitic in composition.

3.1.3 ST30/Hekla 1104 (Hekla 1)

These glass shards closely match the geochemistry of the Hekla 1104 eruption (also known as the Hekla 1 eruption), with an average SiO_2 content of 63-67%. This tephra has previously been found in multiple sites in northern Scandinavia, including the Sammakovuoma peatland in northern Sweden (Watson et al., 2016a) and the Lofoten Islands in arctic Norway (Pilcher et al., 2005); see figure 5.

3.1.4 ST25/Hekla 1158

Several shards with geochemistries similar to Hekla 1158 were found in the Stordalen core at a depth of 23 cm. Tephra from the Hekla 1158 eruption is dacitic in composition, with a silica content of 67-68%. Evidence of this eruption has only recently been found in Europe, in Scandinavian sites in almost all instances (Pilcher et al., 2005; Swindles et al., 2015a).

3.1.5 EA12/Askja 1875

Using the combined age-depth profile (figure 3), it can be seen that the layer in EA falls approximately between 1831 and 1920. A likely candidate for this tephra is therefore the Askja 1875 eruption. Ash from this eruption has previously been found in several sites in Scandinavia (Pilcher et al., 2005; Wastegård, 2008; Watson et al., 2016b), suggesting that the tephra cloud was at least partially carried in a north-easterly heading from the source (the Dyngjufjöll volcanic system). Approximately 0.5 km^3 of rhyolitic tephra was produced during this eruption (Sigurdsson & Sparks, 1981).

3.1.6 NI5 (Unknown tephra)

Using our precise ^{210}Pb chronology, the layer in NI appears to fall between 1971 and 1987, and is therefore of a more uncertain origin as no tephra layers from this period have yet been defined in Scandinavia at the time of writing. As stated above, it was not possible to perform geochemical analysis on these shards; however, several potential source eruptions occurred in Iceland during this period. The Hekla and Krafla volcanic systems both exhibited significant activity, although no tephra from the eruptions occurring at Hekla in 1980 and 1981 has yet been reported outside Iceland. The activity from Krafla was almost exclusively effusive with intermittent phreatic explosions (Global Volcanism Program, 2013), making this an unlikely candidate for distal tephra deposition. A minor subglacial eruption of Grímsvötn occurred in 1983, though again this is unlikely to have produced a sufficient tephra cloud to account for the reported layer (Gronvold & Johannesson, 1984). It is therefore possible that this tephra originated from a non-Icelandic source. Tephra attributed to Alaskan volcanoes has previously been found in northern Scandinavia (Watson et al., 2017), and it has recently been suggested that a previously unidentified tephra found in Svartkälsjärn, Sweden (Watson et al., 2016a) may have originated from the Cascades arc in North America (Plunkett & Pilcher, 2018). These findings indicate that, while Iceland is statistically the most likely source of volcanic ash in Scandinavian peatlands, it may be necessary to look further afield to identify more obscure deposits.

[Figure 4: Geochemical bi-plots of glass shards found in the Marooned and Stordalen cores, showing the geochemical type-data envelopes of the eruptions to which they correlate. Also shown are geochemical envelopes for alternative eruptions occurring within a similar timeframe for comparison. a) ST25, b) ST30, c) MN70, d) MN85. EPMA was performed at the Tephra Analysis Unit, University of Edinburgh.]

4 Discussion

4.1 Tephra transport and preservation

[Figure 5: Spatial distributions within Europe of four tephra layers found in the Abisko peatlands. All four originated at Hekla in southern Iceland, and each has previously been found within Scandinavia. (Swindles et al., 2017)]

While several distinct deposits of tephra were found within the Abisko region, there is poor correlation of tephra preservation across sites, even between cores separated by <10 km. A distinct tephra layer can clearly be found in the Eagle bog site, but is not present at the Craterpool bog, despite the two locations being within 12 km of each other. The same is true of the Marooned and Railway bog sites, which are 9 km apart.

There are a number of components influencing the spatial distribution of tephra over a given deposition area. 'Ash winnowing', referring to the resorting and redeposition of ash sediments, is a phenomenon which has been previously noted in many volcanological studies, and is typically attributed to erosion by wind- or water-based processes. Analysis of distal ash deposits from the 2008 eruption of Chaitén, Chile, for example, showed that unsheltered locations occasionally displayed greater degrees of reworking and variability in deposit thickness, and that these anomalies became more frequent with distance from the eruption source (Watt et al., 2009).

The disparities across the stratigraphic columns shown in our results emphasise how a combination of components can cause extreme variability in glass preservation, even over a relatively small area. Many factors are related to local conditions at the time of deposition, while others relate to broader factors such as regional topography and basin drainage systems. Additionally, eruption conditions at the origin volcano can affect glass composition and ash shard morphology, with implications for tephra preservation and transport respectively (Lowe, 2011). Figure 6 provides a summary of the dominant factors, some of which are explained in greater detail below.

4.2 Site analysis

[Figure 6: Conceptual diagram of factors influencing tephra preservation in Abisko peatlands.]

4.2.1 Local climate and wind currents

The location of Abisko on the leeward side of the Norwegian mountains results in a significant decline in annual rainfall relative to nearby locations on the windward side (Swindles et al., 2015b). While this may decrease the surface runoff in the region, thus decreasing the likelihood of surface redistribution of fallen tephra, it is also thought that precipitation itself may play a crucial role in the deposition of tephra (Davies et al., 2010). Some studies attribute the patchiness of the Hekla 1947 tephra in many areas of Europe to irregular rain- or snowfall (Salmi, 1948; Thorarinsson, 1967).

Another factor to consider when assessing the impact of precipitation on ash preservation is snow cover. Snow provides a ‘shielding’ layer above the underlying peatland, enabling redistribution of deposited tephra through surface wind currents (Bergman et al., 2004). Tephra preserved within snow is also subject to transportation should that snow cover melt during seasonal temperature changes.

The variability of air currents over northern Scandinavia is also likely to be a major controlling factor on tephra deposition in the region. Models suggest that seasonal variability in the dominant air currents has a strong influence on tephra transportation, with strong westerlies at high elevations (>15 km) during autumn and winter, and weak easterlies becoming dominant during spring and summer (Lacasse, 2001). Icelandic eruptions occurring during the latter half of a given year (September-February) are therefore more likely to deposit tephra across Scandinavia. In recent years, however, evidence has emerged that the Earth’s warming climate may have a weakening effect on the polar vortex (Kim et al., 2014). If this is proved to be the case, future patterns of tephra distribution in the northern hemisphere may be altered by continuing climate change.

Additionally, it has been suggested that, under the correct conditions, the combination of a variable wind field and changes to the eruption parameters due to fluctuations in the volcanic system may allow for the creation of discrete deposition patterns for different phases of an eruption (Watt et al., 2009; Stevenson et al., 2012). This may provide an explanation for the unusually uniform major element geochemistries seen in some of the deposits found in Abisko, most notably the ST25 and ST30 deposits, attributed to Hekla 1158 and Hekla 1104 respectively. These shard clusters may represent ashfall from a particular phase of those eruptions, though whether the compositional bias in these deposits occurred during transport or through winnowing and preservation processes is unclear.

Studies of ashfall conducted following the 2008 eruption of Chaitén, Chile indicate a complex pattern of ash deposition which was largely attributed to variable wind fields during the course of the week-long eruption, at least on a proximal scale (Watt et al., 2009; Alfano et al., 2010; Durant et al., 2012). However, variations in wind patterns are typically referenced as a cause of regional-scale depositional variations on the order of hundreds of kilometres, as opposed to the local-scale variations observed in Abisko, which occur across areas of <20 km. While a variable wind field therefore offers a potential explanation for the apparent underrepresentation of many historical Icelandic tephra deposits in Scandinavia relative to the rest of western mainland Europe, shifting regional air currents are unlikely to have caused the erratic preservation pattern observed at Abisko.

4.2.2 Vegetation

Similarly to snow cover, vegetation can provide a shielding effect to underlying sediment. However, a more significant implication for tephra preservation is the effect of root trapping, wherein plant roots capture small packets of sediment, preserving them at a given depth. This has multiple negative consequences for the field of tephrochronology; firstly, the unequal distribution of ash within a given horizon complicates the process of tephra extraction, as it makes the presence of a particular layer at a given depth more uncertain. Additionally, the vertical redistribution of tephra can negatively impact the creation of age-depth profiles for peatlands and lake sediment, as the correlation between tephra layers and dated organic material from the same layer becomes less reliable (Cutler et al., 2016). Dugmore et al., 2018, suggest that uniformly vegetated slopes can produce consistent tephra layers in the stratigraphic record, but areas of sparse or patchy vegetation will result in variability. Many of the Abisko sites were characterised by a uniform top layer of sphagnum moss of between 1-4cm thickness, with intermittent tussocks of thicker vegetation and herbaceous plants such cotton sedge (*Eriophorum angustifolium*). Studies of vegetation succession in the Marooned and Stordalen sites also indicate the variable presence of shrub communities over the past millennium (Gałka et al., 2017), making it likely that root trapping could have interfered with tephra preservation in this region.

Ashfall may also be intercepted by vegetation at a sub-aerial level, such as on leaves and branches. However, the sparseness of larger forms of plant life in most sub-Arctic peatland reduces the influence of this factor in this region.

4.2.3 Topography

A recent study (Dugmore et al., 2018) based on data from Iceland and Washington State, USA, has shown that tephra layers of 1-10 cm thickness can remain stable on slopes <35°, given sufficiently uniform vegetation cover. Slopes of a greater angle are unlikely to produce consistent stratigraphic records, as tephra particles become concentrated in topographic hollows, resulting in down-slope thickening which can cause differences in thickness as great as an order of magnitude between the peak and the base of a slope (Mairs et al., 2006). Down-slope runoff processes can be mitigated by vegetation and ground cover, resulting in small-scale variation within a given layer.

4.2.4 Eruption conditions

Eruption conditions represent a strong control on cryptotephra layers. Very fine ash of the size and density suitable for airborne transport over several thousand kilometres is generated in far greater quantities during explosive silicic eruptions than effusive basaltic eruptions (Rose & Durant, 2009). The effects of ash morphology on airborne tephra transport have been the subject of a great deal of study, as the topic has significant implications for ash cloud modelling techniques. The surface roughness, sphericity and convexity of ash particles all affect the aerodynamic properties of those particles (Riley et al., 2003), which in turn affect the settling velocity, atmospheric residence time, and transport distance. For example, irregular particles with low vesicularities and high surface-to-volume ratios are likely to aggregate due to the high wettability and surface roughness, while flat particles with high long axis to short axis ratios are likely to be transported further from their source (Riley et al., 2003; Cioni et al., 2014). The primary determining factors in ash morphology are magma fragmentation – itself a product of gas content, pressurisation and conduit width, among others – and interaction of the magma and subsequent volcanic plume with water. A greater degree of interaction results in greater fragmentation, giving the tephra a thinner, more concave morphology, with complex implications for transport distance (Freundt & Rosi, 1998).

While a small number of larger (>150 µm) shards were found some samples in the Stordalen and Marooned cores, the vast majority of tephra found in the Abisko region has a thin, wispy morphology with an average length of 50-100 µm and pale colouration, corresponding with the explosive eruptions to which all of the identified ash layers have been assigned.

4.2.5 Other factors

An absence of water outflow is crucial to the successful preservation of a tephra layer. Lakes or fens which have substantial throughflow are typically not suitable for tephrochronological study, as hydrological redistribution of lighter particles is substantially more likely. Dry or impermeable surfaces may also facilitate windblown redistribution of tephra to topographic lows. Particles are therefore preferentially preserved in low areas of damp, permeable terrain. A recent study conducted on thin tephra layers in temperate regions (Blong et al., 2017) suggested that the erosional reworking of tephra layers <300 mm in thickness, as is the case for many European cryptotephra layers, is highly variable even across relatively homogenous sites. These results may indicate the necessity of large sample sizes and the collection of multiple cores within small areas, although in practice this method is likely to become impractical.

5 Conclusions

[1] Six distinct tephra layers, the majority of which are likely to be of Icelandic origin, were recorded in the surveyed Abisko peatland cores.

[2] Using geochemical analysis, we identify shards belonging to the Hekla 4, Hekla 1104, Hekla 1158 and Hekla-Selsund eruptions in Abisko.

[3] From age-depth profiles of two cores, we suggest that the Askja 1875 tephra, and an unidentified, possibly non-Icelandic tephra are present in the Abisko region.

[4] We find very little correlation between tephrostratigraphies of adjacent peat cores, suggesting that local-scale variations in topography, vegetation, snow cover, ground permeability, and other factors significantly influence the preservation of windblown tephra in sub Arctic Sweden.

[5] The variability of tephra preservation across multiple sites within the study area suggests that northern Scandinavian peatlands may be an unreliable source of volcanic ash deposits due to the increased risks of redeposition and secondary transport, further complicating studies into the tephrochronology of the region.

6 Acknowledgements

Claire Cooper acknowledges a Leeds Anniversary Research Scholarship at the University of Leeds, in addition to support from the Climate Research Bursary Fund awarded by the Priestley International Centre for Climate. Elizabeth Watson was funded by NERC funded Doctoral Training Grant NE/K500847/1. We acknowledge the Worldwide University Network (WUN) for funding this project (Project: Arctic Environments, Vulnerabilities and Opportunities). We acknowledge the Abisko Scientific Research Station for assistance with field logistics and Kallax Flyg AB for helicopter support.

Appendix A

Table A.1. Radiocarbon dates of Abisko peat profiles

Site	Lab Code	Depth (cm)	^{14}C Age	1σ Error	Material dated	Cal range 2σ (BP)	Cal Median Age (BP)
Electric	UB2359	17	165	20	*Dicranum bergerii* + *Dicranum elongatum* stems with leaves	166-225	187
	UB2360	22	390	20	*Sphagnum* stems + leaves	434-505	476
Crater Pool I	UB2358	15	860	20	*Sphagnum russowii* stems with leaves	726-796	763
	Poz-80223	22	1110	30	*Sphagnum riparium* stems with leaves	937-1071	1014
Crater Pool II	UB2356	19	160	20	*Betula nana* leaf remains + fruits scale, *Empetrum nigrum* seed remains, *Andromeda polifolia* leaves and seeds, *Sphagnum fuscum* stems with leaves	167-224	187
	UB2357	29	345	20	*Sphagnum fuscum* stems with leaves, *Oxycoccus palustris* leaves, *Betula nana* leaf remains	316-407	386
Railway	UB2366	28	200	20	*Oxycoccus palustris* leaves, *Betula nana* leaf remains, *Sphagnum*	146-189	172

					russowii stems with leaves		
	UB2398_2	40	1240	20	Bulk	1196-1263	1211
Eagle	UB2365	19	130	20	*Dicranum elongatum* stems with leaves, *Pleurozium schreberii* stems with leaves	59-149	119
	UB2397_2	30	1725	25	Bulk	1565-1700	1635
Nikka	UB2363	24	180	20	*Sphagnum fuscum* stems with leaves	142-219	183
	UB2364	30	595	20	*Sphagnum fuscum* stems with leaves	584-647	606
Instrument	UB2361	25	165	20	*Dicranum elongatum* stems with leaves	166-224	187
	UB2362	30	320	20	*Dicranum elongatum* stems with leaves	348-458	387
Stordalen	D-AMS 006366	14	340	24	*Sphagnum*	477-314	388
	D-AMS 006367	17	553	31	*Sphagnum*	640-518	559
Marooned	D-AMS 006368	28	2317	26	Sphagnum, herb epidermis	2360-2211	2342

Table A.2 ^{210}Pb dating of Abisko peat profiles

Site	Cumul. ^{210}Pb_ex inventory (Bq/m2)	±	Residual ^{210}Pb_ex (Bq/m2)	±	Age (year)	YEAR (AD)	±
	19.02	1.68	3632.39	26.67	0.17	2011.83	1.00
	116.57	6.13	3534.84	26.62	1.04	2010.96	1.02
	273.73	8.11	3377.68	25.96	2.50	2009.50	1.06
	504.43	11.26	3146.97	25.41	4.77	2007.23	1.08
	833.18	14.73	2818.22	24.17	8.32	2003.68	1.12
	1263.37	18.20	2388.03	22.23	13.64	1998.36	1.17
	1942.68	21.82	1708.73	19.49	24.39	1987.61	1.25
	2485.15	23.74	1166.26	15.33	36.65	1975.35	1.35
	3073.40	25.72	578.01	12.15	59.19	1952.81	1.61
	3359.58	26.35	291.83	7.05	81.14	1930.86	1.75
	3582.02	26.53	69.39	4.14	127.27	1884.73	2.89
	3651.40	26.67	0.00	2.76			
	3651.40	26.85					
Marooned	3611.87	26.91					

	3618.02	31.04					
	3556.55	33.89					
	47.57	4.29	3602.81	45.06	0.42	2011.58	1.01
	166.11	7.75	3484.27	44.85	1.50	2010.50	1.04
	553.84	18.48	3096.54	44.38	5.28	2006.72	1.10
	1239.81	25.69	2410.57	41.09	13.33	1998.67	1.25
	1923.16	30.09	1727.22	37.01	24.03	1987.97	1.43
	2521.79	40.57	1128.59	33.53	37.70	1974.30	1.71
	3064.50	43.78	585.89	19.60	58.75	1953.25	1.97
	3441.33	44.64	209.05	10.63	91.84	1920.16	2.59
	3650.38	45.06	0.00	6.09			
	3650.38	45.48					
	3606.77	45.52					
	3580.58	45.59					
	3511.91	45.65					
	3254.74	45.99					
	2968.36	47.14					
	2868.03	48.93					
Eagle	2579.98	51.08					
	129.65	12.70	2517.20	28.58	1.61	2010.39	1.02
	328.28	16.64	2318.57	25.61	4.25	2007.75	1.16
	600.43	18.59	2046.42	23.24	8.26	2003.74	1.22
	1018.88	20.87	1627.98	21.71	15.61	1996.39	1.28
	1599.29	23.67	1047.56	19.53	29.77	1982.23	1.44
	1971.58	27.37	675.27	16.03	43.87	1968.13	1.64
	2248.59	28.20	398.26	8.23	60.82	1951.18	1.65
	2455.75	28.40	191.10	4.65	84.40	1927.60	1.80
	2584.36	28.51	62.50	3.23	120.30	1891.70	2.66
	2646.85	28.58	0.00	2.05			
	2646.85	28.75					
	2618.05	29.25					
	2607.31	29.73					
	2594.90	31.04					
Nikka	2556.27	31.43					
	129.65	12.70	2517.20	28.58	1.61	2010.39	1.02
	328.28	16.64	2318.57	25.61	4.25	2007.75	1.16
	600.43	18.59	2046.42	23.24	8.26	2003.74	1.22
	1018.88	20.87	1627.98	21.71	15.61	1996.39	1.28
	1599.29	23.67	1047.56	19.53	29.77	1982.23	1.44
	1971.58	27.37	675.27	16.03	43.87	1968.13	1.64
	2248.59	28.20	398.26	8.23	60.82	1951.18	1.65
	2455.75	28.40	191.10	4.65	84.40	1927.60	1.80
	2584.36	28.51	62.50	3.23	120.30	1891.70	2.66
	2646.85	28.58	0.00	2.05			
	2646.85	28.75					
	2618.05	29.25					
	2607.31	29.73					
	2594.90	31.04					
Stordalen	2556.27	31.43					

Appendix B

Table B.1. Non-normalised major element glass geochemistry of Abisko peat profiles

Core	Depth (cm)	SiO_2	TiO_2	Al_2O_3	FeO	MnO	MgO	CaO	Na_2O	K_2O	P_2O_5	Total
Marooned	85	70.54	0.45	13.10	4.65	0.19	0.18	1.53	4.89	3.52	0.05	99.09
		76.16	0.24	11.91	2.06	0.08	0.07	0.90	4.19	3.03	0.03	98.69
		73.40	0.28	14.28	3.43	0.12	0.32	2.41	4.91	1.95	0.05	101.19
		71.93	0.24	13.25	2.98	0.12	-0.20	1.95	5.25	2.40	0.03	97.96
		63.12	0.85	14.63	7.49	0.23	0.89	4.45	4.17	1.87	0.28	97.98
		64.73	0.85	15.19	7.59	0.24	0.90	4.55	4.78	1.67	0.29	100.75
		73.99	0.14	12.80	2.01	0.08	0.05	1.35	5.02	2.90	0.01	98.38
		66.65	0.52	15.15	4.41	0.20	0.34	1.87	5.54	3.88	0.07	98.65
		72.96	0.13	12.14	1.94	0.09	0.03	1.18	4.67	2.82	0.00	95.98
		66.40	0.57	15.02	5.22	0.17	0.45	3.66	5.69	1.59	0.16	98.92
		66.23	0.59	15.03	4.04	0.11	0.31	3.87	5.64	1.35	0.19	97.34
		71.16	0.24	13.29	3.09	0.11	0.13	2.06	5.06	2.48	0.02	97.67
		71.96	0.23	12.95	2.84	0.11	0.10	1.87	4.71	2.58	0.02	97.41
		63.02	1.18	15.07	7.17	0.20	1.38	4.75	4.41	1.57	0.40	99.09
		64.28	1.18	14.04	7.17	0.21	1.35	4.58	4.48	1.52	0.39	99.11
		75.55	0.20	12.23	1.73	0.07	0.06	1.34	4.34	2.75	0.03	98.36
Stordalen	25	69.57	0.46	13.51	5.23	0.14	0.34	2.34	4.97	2.88	0.10	99.54
		69.36	0.42	15.53	4.17	0.11	0.19	3.01	5.34	2.44	0.10	100.68
		69.26	0.50	14.28	4.83	0.19	0.24	2.81	5.49	2.54	0.10	100.25
		68.79	0.47	15.19	5.09	0.15	0.40	3.29	5.47	2.05	0.09	100.99
		68.72	0.46	15.23	5.52	0.17	0.43	3.13	5.27	2.30	0.11	101.34
		68.68	0.47	15.41	5.46	0.17	0.47	3.15	5.12	2.32	0.10	101.35
		68.40	0.48	14.09	5.48	0.19	0.42	3.03	5.06	2.42	0.10	99.68
		68.23	0.48	14.53	5.48	0.17	0.48	3.33	5.16	2.31	0.09	100.26
		68.11	0.47	15.35	5.70	0.18	0.46	2.96	5.30	2.38	0.10	101.01
		67.90	0.47	14.36	5.31	0.18	0.44	3.14	5.54	2.30	0.11	99.75
		67.84	0.48	14.88	5.75	0.17	0.45	3.22	5.12	2.31	0.11	100.32
		67.84	0.47	14.52	5.83	0.15	0.46	3.28	4.81	2.31	0.12	99.77
		67.80	0.48	15.01	5.75	0.19	0.50	3.02	4.78	2.26	0.08	99.97
		67.66	0.46	15.06	5.70	0.18	0.46	2.94	5.71	2.24	0.09	100.51
		67.62	0.45	14.22	5.39	0.14	0.50	3.02	5.44	2.41	0.11	99.30
		67.60	0.46	14.83	5.76	0.16	0.44	3.14	5.43	2.35	0.10	100.29
		67.60	0.48	15.22	5.65	0.19	0.44	3.14	5.09	2.39	0.10	100.31
		67.39	0.46	15.04	6.06	0.17	0.46	3.02	5.55	2.30	0.11	100.56
		67.22	0.45	14.85	5.61	0.17	0.48	3.11	5.39	2.32	0.11	99.71
		67.11	0.41	16.93	4.25	0.15	0.34	3.88	5.87	1.97	0.09	101.00
		65.41	0.07	13.85	5.66	0.11	0.41	3.16	4.04	2.19	0.07	95.20
		64.71	0.27	20.15	3.10	0.07	0.31	5.19	6.36	1.32	0.06	101.54
Stordalen	30	67.63	0.38	16.11	4.01	0.16	0.26	1.78	5.73	4.18	0.05	100.29
		67.49	0.40	15.75	4.05	0.19	0.27	1.82	6.16	4.22	0.06	100.40
		67.48	0.39	16.25	4.23	0.18	0.24	1.85	6.22	4.21	0.06	101.12
		67.41	0.39	15.78	4.42	0.16	0.33	1.76	5.92	4.16	0.05	100.38
		67.28	0.47	15.85	4.69	0.19	0.46	2.05	5.97	3.94	0.09	101.01
		67.20	0.43	15.84	4.75	0.20	0.36	2.09	5.73	4.11	0.64	100.76
		66.98	0.34	15.68	3.76	0.15	0.23	1.71	6.01	4.21	0.06	99.12
		66.96	0.46	16.59	4.48	0.19	0.40	2.24	5.99	4.13	0.08	101.52
		66.76	0.43	15.94	4.34	0.16	0.37	1.98	6.14	4.07	0.06	100.25
		66.66	0.43	16.64	4.14	0.17	0.32	1.96	5.87	4.02	0.07	100.28
		66.50	0.36	16.14	4.28	0.15	0.28	1.58	6.14	4.28	0.06	99.73

		66.44	0.33	14.26	3.60	0.15	0.19	1.63	5.64	4.29	0.04	96.56
		66.27	0.41	15.63	4.34	0.18	0.35	1.99	6.25	4.06	0.07	99.53
		65.85	0.47	14.11	5.66	0.28	0.66	2.73	5.49	4.12	0.08	99.46
		65.83	0.57	16.08	5.60	0.23	0.57	2.43	5.74	3.78	0.12	100.94
		65.73	0.38	15.60	4.07	0.16	0.31	1.80	5.92	4.27	0.07	98.31
		65.41	0.46	15.62	4.53	0.18	0.31	1.96	6.07	3.98	0.07	98.60
		65.13	0.46	15.79	4.61	0.17	0.34	2.12	6.13	3.92	0.08	98.74
		64.89	0.40	15.78	4.17	0.18	0.31	1.89	5.89	4.18	0.07	97.76
		63.34	0.43	15.82	4.25	0.16	0.31	1.87	5.71	3.95	0.06	95.91
Marooned	70	72.02	0.62	14.51	2.45	0.16	0.53	1.71	6.08	2.84	0.10	100.96
		64.63	0.77	15.68	5.58	0.24	0.54	2.65	6.43	3.65	0.16	100.27
		72.73	0.64	13.28	3.17	0.15	0.69	2.61	4.65	1.71	0.13	99.73
		71.16	0.25	13.54	3.02	0.12	0.12	1.98	4.66	2.36	0.03	97.28
		70.33	0.31	13.18	3.82	0.17	0.11	1.29	4.87	5.10	0.04	99.24
		65.73	0.67	14.49	6.32	0.21	0.58	3.43	4.99	1.95	0.20	98.55
		71.67	0.25	13.34	3.00	0.12	0.13	1.85	5.08	2.42	0.02	97.90
		71.40	0.23	13.42	2.98	0.14	0.02	1.79	5.64	2.78	0.01	98.42
		64.60	0.77	14.05	7.17	0.23	0.78	3.93	4.40	1.67	0.24	97.82
		72.28	0.24	13.55	3.13	0.12	0.11	1.92	5.84	2.42	0.03	99.63

Table B.2 EMPA of Lipari and BCR-2G glass standards prior to Abisko glass shard analysis

DataSet	SiO2	TiO2	Al2O3	FeO	MnO	MgO	CaO	Na2O	K2O	P2O5	Total	Comment	Mea Z
1 / 1 .	55.20	2.30	13.56	12.15	0.20	3.60	6.93	3.21	1.79	0.36	99.29	BCR2g	12.7
2 / 1 .	54.41	2.26	13.38	12.48	0.17	3.72	7.13	3.28	1.74	0.38	98.96	BCR2g	12.7
3 / 1 .	54.54	2.26	13.16	12.58	0.21	3.75	6.91	3.32	1.88	0.39	99.00	BCR2g	12.7
4 / 1 .	53.96	2.26	13.23	12.38	0.20	3.77	7.03	3.52	1.79	0.38	98.51	BCR2g	12.6
5 / 1 .	74.43	0.07	12.70	1.76	0.07	0.04	0.81	4.18	5.23	0.00	99.30	Lipari	11.2
6 / 1 .	74.04	0.08	12.68	1.63	0.07	0.04	0.71	4.16	4.96	0.01	98.36	Lipari	11.1
7 / 1 .	74.78	0.07	12.99	1.59	0.07	0.06	0.72	4.27	5.21	0.00	99.76	Lipari	11.2
8 / 1 .	74.50	0.07	12.80	1.65	0.07	0.02	0.79	4.01	5.24	0.00	99.15	Lipari	11.2
9 / 1 .	54.11	2.26	13.23	12.50	0.18	3.69	6.99	3.21	1.86	0.36	98.40	BCR2g	12.6
10 / 1 .	54.70	2.27	13.33	12.72	0.20	3.76	7.09	3.42	1.76	0.36	99.60	BCR2g	12.8
11 / 1 .	54.92	2.26	13.41	12.62	0.19	3.66	7.11	3.42	1.81	0.38	99.77	BCR2g	12.8
12 / 1 .	54.22	2.28	13.08	11.70	0.20	3.80	7.00	3.25	1.86	0.35	97.74	BCR2g	12.4

Appendix C

Table C.1 Site information

Site name	Codes	Latitude (°N)	Longitude (°E)	Peatland type	Number of samples	Water table depth range (cm)	pH range
Craterpool	P1-7	68°19′10.1″	19°51′27.2″	Palsa	7	− 5 to 45	3.76–4.77
Eagle	E1-6	68°21′56.5″	19°35′02.9″	Fen and bog	6	0 to 29	4.52–6.74
Electric	L1-6	67°51′56.1″	19°22′06.4″	Palsa	6	0 to 45	3.66–6.95

Site name	Codes	Latitude (°N)	Longitude (°E)	Peatland type	Number of samples	Water table depth range (cm)	pH range
Instrument	I1-6	68°11′52.4″	19°45′56.2″	Palsa	6	0 to 36	3.43–5.32
Marooned	M1-7	67°57′24.0″	19°59′11.4″	Fen and bog	7	− 1 to 29	3.24–4.21
Nikka	N1-6	67°52′02.2″	19°10′42.5″	Fen and bog	6	− 1 to 40	4.02–5.27
Railway	R1-7	68°05′12.6″	19°49′52.9″	Palsa	7	0 to 40	3.25–6.35
Stordalen	S1-40	68°21′24.3″	19°02′53.5″	Palsa and fen	40	− 7 to 50	2.99–3.80

References

1. Alatalo, J.M., Jägerbrand, A.K. and Molau, U. 2016. Impacts of different climate change regimes and extreme climatic events on an alpine meadow community. Scientific Reports, 6 (21720)
2. Alfano, F., Bonadonna, C., Volentik, A.C., Connor, C.B., Watt, S.F., Pyle, D.M. and Connor, L.J., 2011. Tephra stratigraphy and eruptive volume of the May, 2008, Chaitén eruption, Chile. Bulletin of Volcanology, 73(5), pp.613-630.
3. Appleby, P. G. 2001. Chronostratigraphic techniques in recent sediments *in* Tracking environmental change using lake sediments Vol. 2: Physical and geochemical methods (eds Last, W. M. & Smol, J. P.) 171–203. Springer.
4. Bergman, J., Wastegård, S., Hammarlund, D., Wohlfarth, B. and Roberts, S. J. 2004. Holocene tephra horizons at Klocka Bog, west-central Sweden: aspects of reproducibility in subarctic peat deposits. J. Quaternary Sci., 19: 241–249. doi:10.1002/jqs.833
5. Blockley, S.P.E. et al. 2005. A new and less destructive laboratory procedure for the physical separation of distal glass tephra shards from sediments. Quat. Sci. Rev., 24, pp. 1952-1960
6. Blong, R., Enright, N., and Grasso, P. 2017. Preservation of thin tephra. Journal of Applied Volcanology, 6. https://doi.org/10.1186/s13617-017-0059-4
7. Bourne, A.J., Abbott, P.M., Albert, P.G., Cook, E., Pearce, N.J., Ponomareva, V., Svensson, A. and Davies, S.M., 2016. Underestimated risks of recurrent

long-range ash dispersal from northern Pacific Arc volcanoes. Scientific Reports, 629837.

8. Cadle, R.D., Kiang, C.S. and Louis, J.-F. 1976. The global scale dispersion of the eruption clouds from major volcanic eruptions. Journal of Geophysical Research, 81, 3125-3132
9. Callaghan, T.V., Bergholm, F., Christensen, T.R., Jonasson, C., Kokfelt, U., Johansson, M., 2010. A new climate era in the sub-Arctic: Accelerating climate changes and multiple impacts. Geophys Res Lett 37, 14705.
10. Camill, P. 1999. Patterns of boreal permafrost peatland vegetation across environmental gradients sensitive to climate warming. Canadian Journal of Botany, 77 (5), 721-733
11. Camill, P. 2004. Permafrost thaw accelerates in boreal peatlands during late-20th century climate warming. Climatic Change, 68 (1-2), 135-152
12. Cioni, R. et al. 2014. Insights into the dynamics and evolution of the 2010 Eyjafjallajökull summit eruption (Iceland) provided by volcanic ash textures. Earth and Planetary Science Letters, 394, 111-123
13. Cutler, N.A., Bailey, R.M., Hickson, K.T., Streeter, R.T., and Dugmore, A.J., 2016. Vegetation structure influences the retention of airfall tephra in a sub-Arctic landscape. Progress in Physical Geography: Earth and Environment , 40 (5), 661-675
14. Davies, S.M. et al. 2010. Widespread dispersal of Icelandic tephra: how does the Eyjafjöll eruption of 2010 compare to past Icelandic events? Journal of Quaternary Science: Rapid Communication, 25 (5), 605-611
15. Dugmore, A. J., and Newton, A. J. 1992. Thin tephra layers in peat revealed by X-radiography. J. Archaeol. Sci., 19, 163–170, doi:10.1016/0305-4403(92)90047-7.
16. Dugmore, A., Streeter, R. and Cutler, N. 2018. The role of vegetation cover and slope angle in tephra layer preservation and implications for Quaternary tephrostratigraphy. Palaeogeography, Palaeoclimatology, Palaeoecology, 489, 105-116
17. Durant, A.J., Villarosa, G., Rose, W.I., Delmelle, P., Prata, A.J. and Viramonte, J.G., 2012. Long-range volcanic ash transport and fallout during the 2008

eruption of Chaitén volcano, Chile. Physics and Chemistry of the Earth, Parts A/B/C, 45, 50-64.

18. Freundt, A. and Rosi, M. 1998. From magma to tephra : modelling physical processes of explosive volcanic eruptions. 1st ed. Elsevier, Published Amsterdam ; New York. ISBN: 0444829598
19. Gałka, M. et al. 2017. Vegetation Succession, Carbon Accumulation and Hydrological Change in Subarctic Peatlands, Abisko, Northern Sweden. Permafrost and Periglac. Process., 28, 589–604. doi: 10.1002/ppp.1945.
20. Global Volcanism Program, 1998. Report on Grimsvotn (Iceland). In Wunderman, R (ed.), Bulletin of the Global Volcanism Network, 23:11. Smithsonian Institution. https://dx.doi.org/10.5479/si.GVP.BGVN199811-373010.
21. Global Volcanism Program, 2000. Report on Hekla (Iceland). In Wunderman, R (ed.), Bulletin of the Global Volcanism Network, 25:2. Smithsonian Institution. https://dx.doi.org/10.5479/si.GVP.BGVN200002-372070.
22. Global Volcanism Program, 2013. Krafla (373080) In Volcanoes of the World, v. 4.6.6. Venzke, E (ed.). Smithsonian Institution. Downloaded 16 Feb 2018 (http://volcano.si.edu/volcano.cfm?vn=373080). https://dx.doi.org/10.5479/si.GVP.VOTW4-2013
23. Gronvold, K. and Jóhannesson, H., 1984. Eruption in Grímsvötn 1983; course of events and chemical studies of the tephra. Jökull, (34), 1-8.
24. Hayward, C., 2012. High spatial resolution electron probe microanalysis of tephras and melt inclusions without beam-induced chemical modification. The Holocene 22, 119-125.
25. Kim, B.-M. et al. 2014. Weakening of the stratospheric polar vortex by Arctic sea-ice loss. Nature Communications, 5 (4646) doi:10.1038/ncomms5646
26. Lacasse, C. 2001. Influence of climate variability on the atmospheric transport of Icelandic tephra in the subpolar North Atlantic. Global and Planetary Change, 29 (1-2), 31-55
27. Lai, D.Y.F., 2009. Methane dynamics in northern peatlands: a review. Pedosphere, 19(4), 409-421.

28. Lane, C.S., Cullen, V.L., White, D., Bramham-Law, C.W.F. and Smith, V.C. 2014. Cryptotephra as a dating and correlation tool in archaeology. Journal of Archaeological Science, 42, 42-50
29. Lane, C.S., Lowe, D.J., Blockley, S.P.E., Suzuki, T. and Smith, V.C. 2017. Advancing tephrochronology as a global dating tool: Applications in volcanology, archaeology and palaeoclimatic research. Quaternary Geochronology, 40, 1-7
30. Larsen, G . 1993 . Nokkur orð um Kötlugjósku. In Larsen, G., ed. Kötlustefna, March 27-29, ágrip erinda (abstracts). Reykjavík , Raunvisindastofnun, 6- 7. (Háskólans Fjölrit RH-3-93.)
31. Lett, S. 2017. Mosses as mediators of climate change: implications for tree seedling establishment in the tundra. Doctoral thesis, Umeå University
32. Lowe, D.J. 2011. Tephrochronology and its application: A review. Quaternary Geochronology, 6(2), 107-153
33. Lundin, E.J. et al. 2016. Is the subarctic landscape still a carbon sink? Evidence from a detailed catchment balance. Geophysical Research Letters, 43 (5), 1988-1995
34. Mairs, K.A., Church, M.J., Dugmore, A.J., Sveinbjarnardóttir, G., Arneborg, J., and Grønnow, B. 2006. Degrees of success: evaluating the environmental impacts of successful long term settlement in south Iceland. In The Dynamics of Northern Societies. PNM, Publications from the National Museum, Studies in Archaeology and History, 10, 363-372. IBSN: 87-7602-052-5
35. Osterkamp, T.E. and Romanovsky, V.E. 1999. Evidence for warming and thawing of discontinuous permafrost in Alaska. Permafrost and Periglacial Processes, 10 (1), 17-37
36. Palais, J.M., Germani, M.S. and Zielinski, G.A. 1992. Inter-hemispheric transport of volcanic ash from a 1259 A.D. volcanic eruption to the Greenland and Antarctic ice sheets. Geophysical Research Letters, 19 (8), 801-804
37. Pilcher, J.R. and Hall, V.A. 1996. Tephrochronological studies in northern England. The Holocene, 6 (1), 100-105.

38. Pilcher, J., Bradley, R.S., Francus, P. and Anderson, L., 2005. A Holocene tephra record from the Lofoten Islands, arctic Norway. Boreas, 34(2), pp.136-156.
39. Plunkett, G. and Pilcher, J. 2018. Defining the potential source region of volcanic ash in northwest Europe during the Mid- to Late Holocene. Earth Science Reviews, 179, 20-37
40. Ravikumar, S., Surekha, R., Thavarajah, R. 2014. Mounting media: An overview. J. NTR. Univ. Health Sci., 3, Suppl S1:1-8
41. Reimer, P.J., et al., 2013. IntCal13 and Marine13 radiocarbon age calibration curves 0–50,000 years cal BP. *Radiocarbon*, *55*(4), pp.1869-1887.
42. Riley, C. M., Rose, W. I., and Bluth, G. J. S. 2003. Quantitative shape measurements of distal volcanic ash. J. Geophys. Res., 108, 2504, doi:10.1029/2001JB000818, B10.
43. Rose, W.I. and Durant, A.J., 2009. Fine ash content of explosive eruptions. Journal of Volcanology and Geothermal Research, 186(1-2), 32-39.
44. Salmi, M. 1948. The Hekla ash falls in Finland. Suomen Geologinen Seura 21: 87–96.
45. Schuur, E.A.G. and Abbott, B. 2011. Climate change: High risk of permafrost thaw. Nature, 480, 32-33
46. Sigurdsson, H., and Sparks, R.S.J., 1981. Petrology of rhyolitic and mixed magma ejecta from the 1875 eruption of Askja, Iceland. Journal of Petrology, 22(1), 41-84.
47. Stevenson, J.A., et al. 2012. Distal deposition of tephra from the Eyjafjallajökull 2010 summit eruption. Journal of Geophysical Research: Solid Earth, 117(B9).
48. Stivrins N., Wulf S., Wastegard S., Lind E.M., Alliksaar T., Gałka M., Andersen T.J., Heinsalu A., Seppa H., Veski S., 2016. Detection of the Askja AD 1875 cryptotephra in Latvia, Eastern Europe. Journal of Quaternary Science, 31, 437-441.
49. Swindles, G.T., De Vleeschouwer F. and Plunkett, G. 2010. Dating peat profiles using tephra: stratigraphy, geochemistry and chronology. Mires and Peat, 7 (5), 1-9

50. Swindles, G.T., Lawson, I.T., Savov, I.P., Connor, C.B. and Plunkett, G. 2011. A 7000 yr perspective on volcanic ash clouds affecting northern Europe. Geology, 39, 887-890
51. Swindles, G.T. et al. 2015a. Evaluating the use of testate amoebae for palaeohydrological reconstruction in permafrost peatlands. Palaeogeography, Palaeoclimatology,Palaeoecology, 424, 111–122. https://doi.org/10.1016/j.palaeo.2015.02.004
52. Swindles, G.T., et al. 2015b. The long-term fate of permafrost peatlands under rapid climate warming. Scientific Reports 5, 17951.
53. Swindles, G.T., Watson, E.J., Savov, I.P., Cooper, C.L., Lawson, I.T., Schmidt, A. and Carrivick, J.L. 2017. Holocene volcanic ash database for Northern Europe. Database. DOI: 10.13140/RG.2.2.11395.60966
54. Swindles, G.T., et al. 2018. Climatic control on Icelandic volcanic activity during the mid-Holocene. Geology, 46, 47-50
55. Thorarinsson, S. 1967. The eruptions of Hekla in historical times: A tephrochronological study. In The Eruption of Hekla 1947–1948,Einarsson T, Kjartansson G, Thorarinsson S (eds). Societas Scientiarum Islandica: Reykjavik; 1–170.
56. Vikhamer-Schuler, D., Isaksen, K., Haugen, J.E. and Tømmervik, H. 2016. Changes in Winter Warming Events in the Nordic Arctic Region. Journal of Climate, 29 (17), 6223-6244
57. Wastegård, S., Rundgren, M., Schoning, K., Andersson, S., Björck, S., Borgmark, A. and Possnert, G., 2008. Age, geochemistry and distribution of the mid-Holocene Hekla-S/Kebister tephra. The Holocene, 18(4), 539-549.
58. Watson, E.J., Swindles, G.T., Lawson, I.T. and Savov, I.P. 2015. Spatial variability of tephra and carbon accumulation in a Holocene peatland. Quaternary Science Reviews, 124, 248-264
59. Watson, E.J., Swindles, G.T., Lawson, I.T. and Savov, I.P. 2016a. Do peatlands or lakes provide the most comprehensive distal tephra records? Quaternary Science Reviews, 139, 110-128
60. Watson, E.J., Swindles, G.T., Stevenson, J.A., Savov, I. and Lawson, I.T. 2016b. The transport of Icelandic volcanic ash: Insights from northern European

cryptotephra records. Journal of Geophysical Research: Solid Earth, 121(10), 7177-7192

61. Watson, E.J., Swindles, G.T., Savov, I., Lawson, I.T., Connor, C. and Wilson, J. 2017. Estimating the frequency of volcanic ash clouds over northern Europe. Earth and Planetary Science Letters 460, 41-49.
62. Watt, S.F., Pyle, D.M., Mather, T.A., Martin, R.S. and Matthews, N.E., 2009. Fallout and distribution of volcanic ash over Argentina following the May 2008 explosive eruption of Chaitén, Chile. Journal of Geophysical Research: Solid Earth, 114(B4).
63. Whittle, A. and Gallego-Sala, A.V. 2016. Vulnerability of the peatland carbon sink to sea level rise. Scientific Reports, 6, 28758.
64. Woollings, T., Hannachi, A. and Hoskins, B. 2010. Variability of the North Atlantic eddy-driven jet stream. Quarterly Journal of the Royal Meteorological Society, 136 (649), 856-868

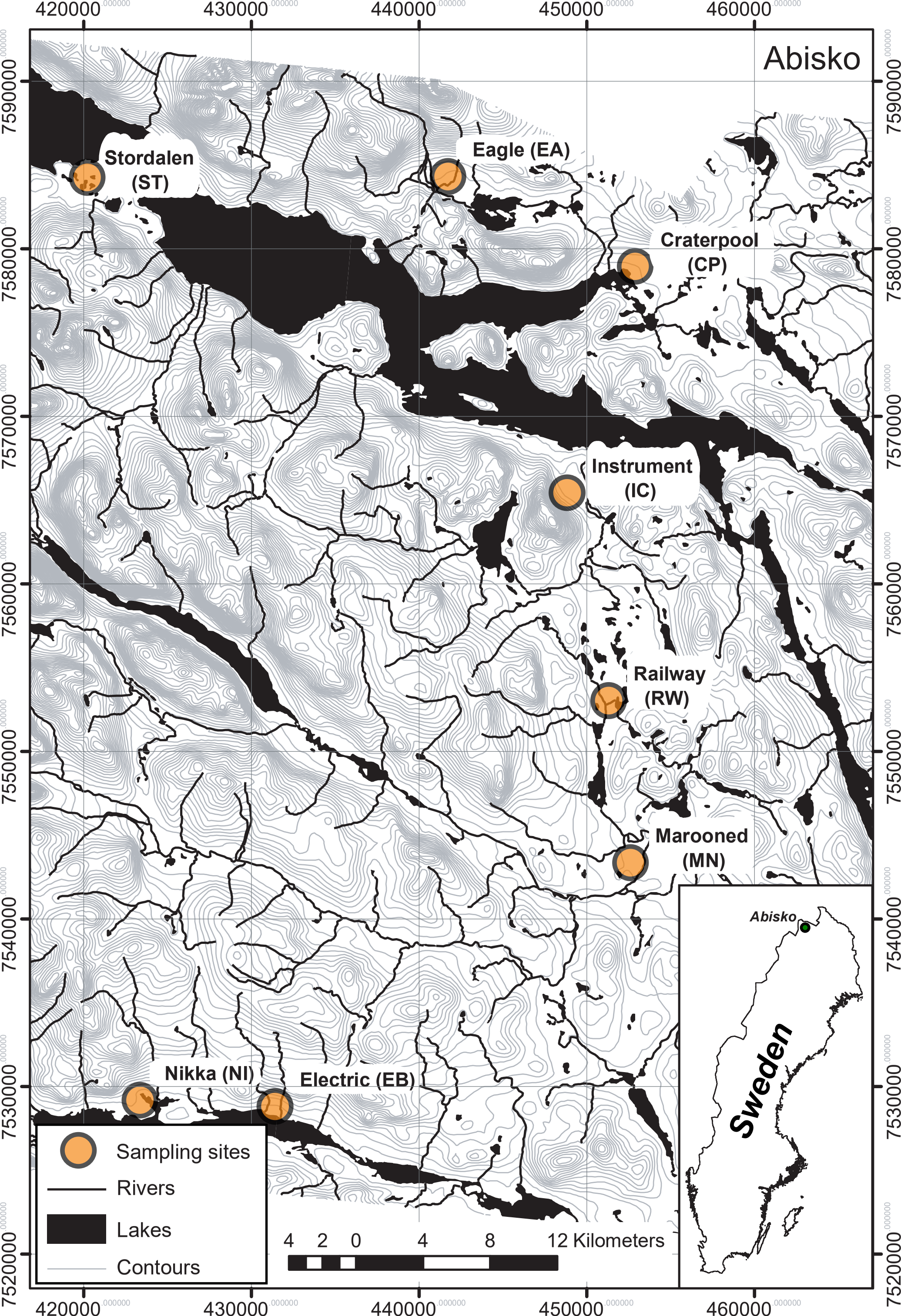
Abisko
Stordalen (ST)
Eagle (EA)
Craterpool (CP)
Instrument (IC)
Railway (RW)
Marooned (MN)
Nikka (NI)
Electric (EB)
Sampling sites
Rivers
Lakes
Contours
4 2 0 4 8 12 Kilometers
Abisko
Sweden
420000
430000
440000
450000
460000
7520000
7530000
7540000
7550000
7560000
7570000
7580000
7590000

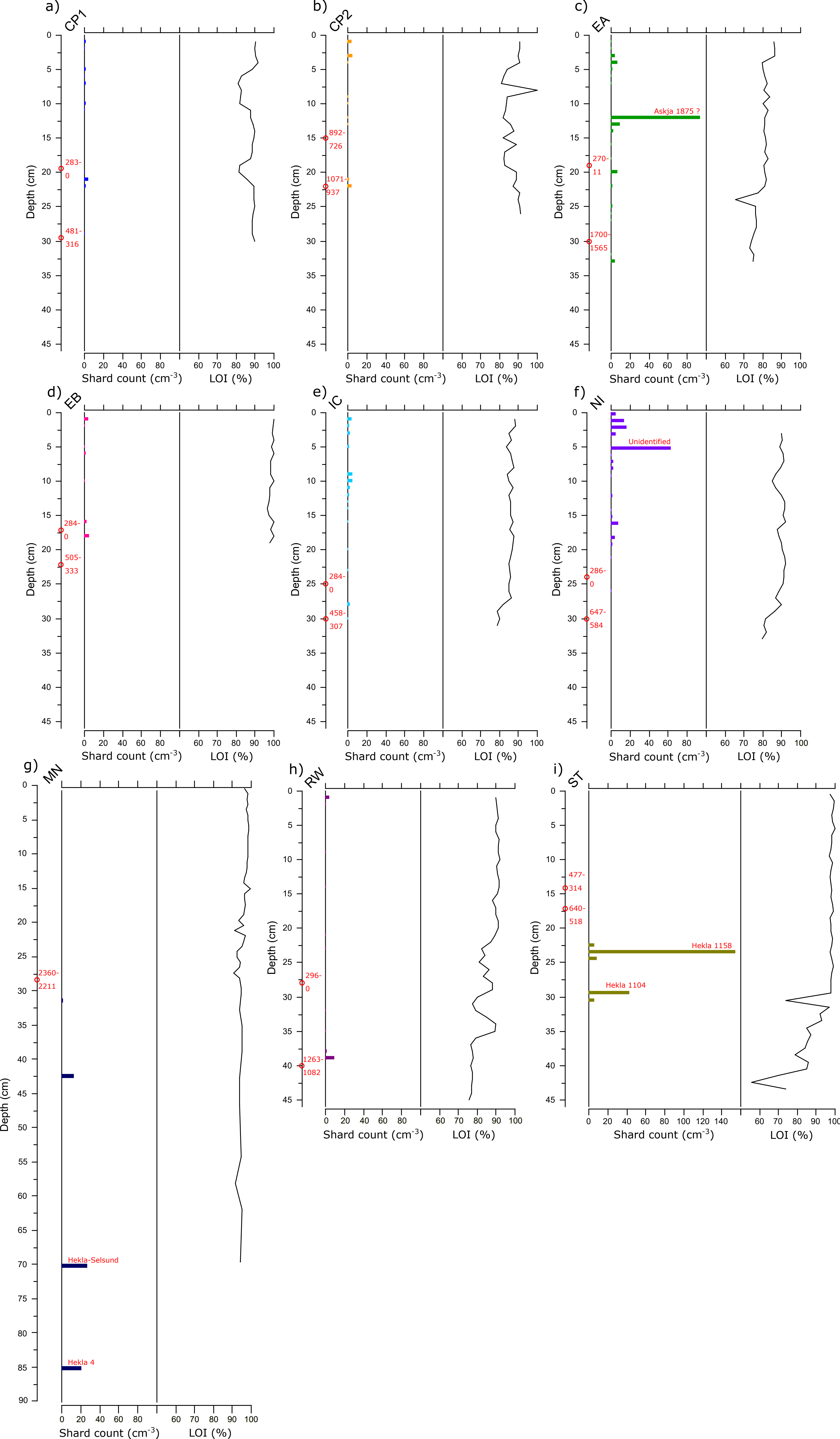

a) CP1
b) CP2
c) EA
d) EB
e) IC
f) NI
g) MN
h) RW
i) ST
Depth (cm)
Shard count (cm^{-3})
LOI (%)
283-
0
481-
316
892-
726
1071-
937
Askja 1875 ?
270-
11
1700-
1565
284-
0
505-
333
284-
0
458-
307
Unidentified
286-
0
647-
584
2360-
2211
Hekla-Selsund
Hekla 4
296-
0
1263-
1082
477-
314
640-
518
Hekla 1158
Hekla 1104

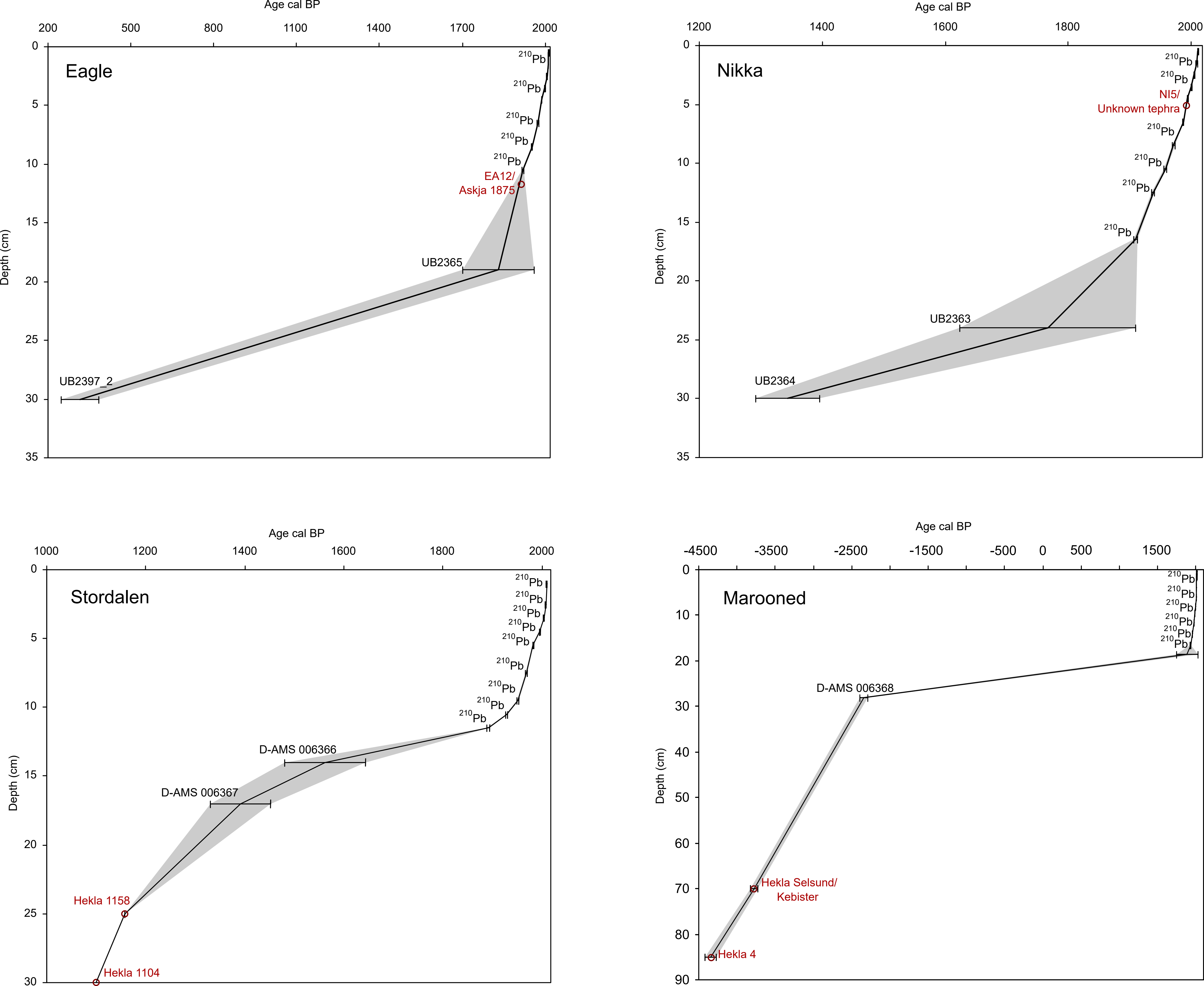

Eagle
Age cal BP
Depth (cm)
210Pb
EA12/
Askja 1875
UB2365
UB2397_2
Nikka
NI5/
Unknown tephra
UB2363
UB2364
Stordalen
D-AMS 006366
D-AMS 006367
Hekla 1158
Hekla 1104
Marooned
D-AMS 006368
Hekla Selsund/
Kebister
Hekla 4

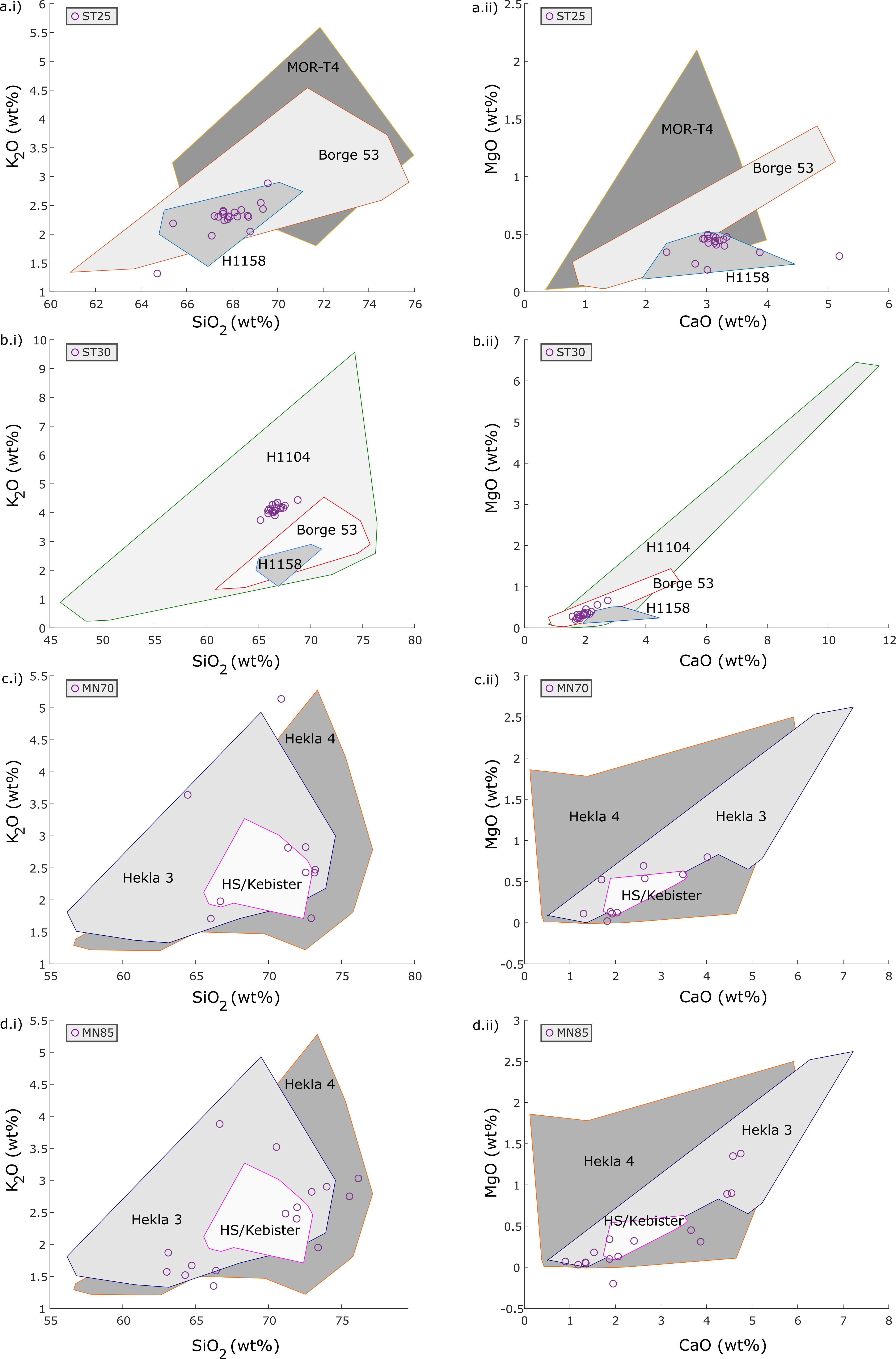
a.i)
ST25
MOR-T4
Borge 53
H1158
K_2O (wt%)
SiO_2 (wt%)
a.ii)
ST25
MOR-T4
Borge 53
H1158
MgO (wt%)
CaO (wt%)
b.i)
ST30
H1104
Borge 53
H1158
K_2O (wt%)
SiO_2 (wt%)
b.ii)
ST30
H1104
Borge 53
H1158
MgO (wt%)
CaO (wt%)
c.i)
MN70
Hekla 4
Hekla 3
HS/Kebister
K_2O (wt%)
SiO_2 (wt%)
c.ii)
MN70
Hekla 4
Hekla 3
HS/Kebister
MgO (wt%)
CaO (wt%)
d.i)
MN85
Hekla 4
Hekla 3
HS/Kebister
K_2O (wt%)
SiO_2 (wt%)
d.ii)
MN85
Hekla 3
Hekla 4
HS/Kebister
MgO (wt%)
CaO (wt%)

Hekla 4

Hekla S/Kebister

Hekla 1104

Hekla 1158

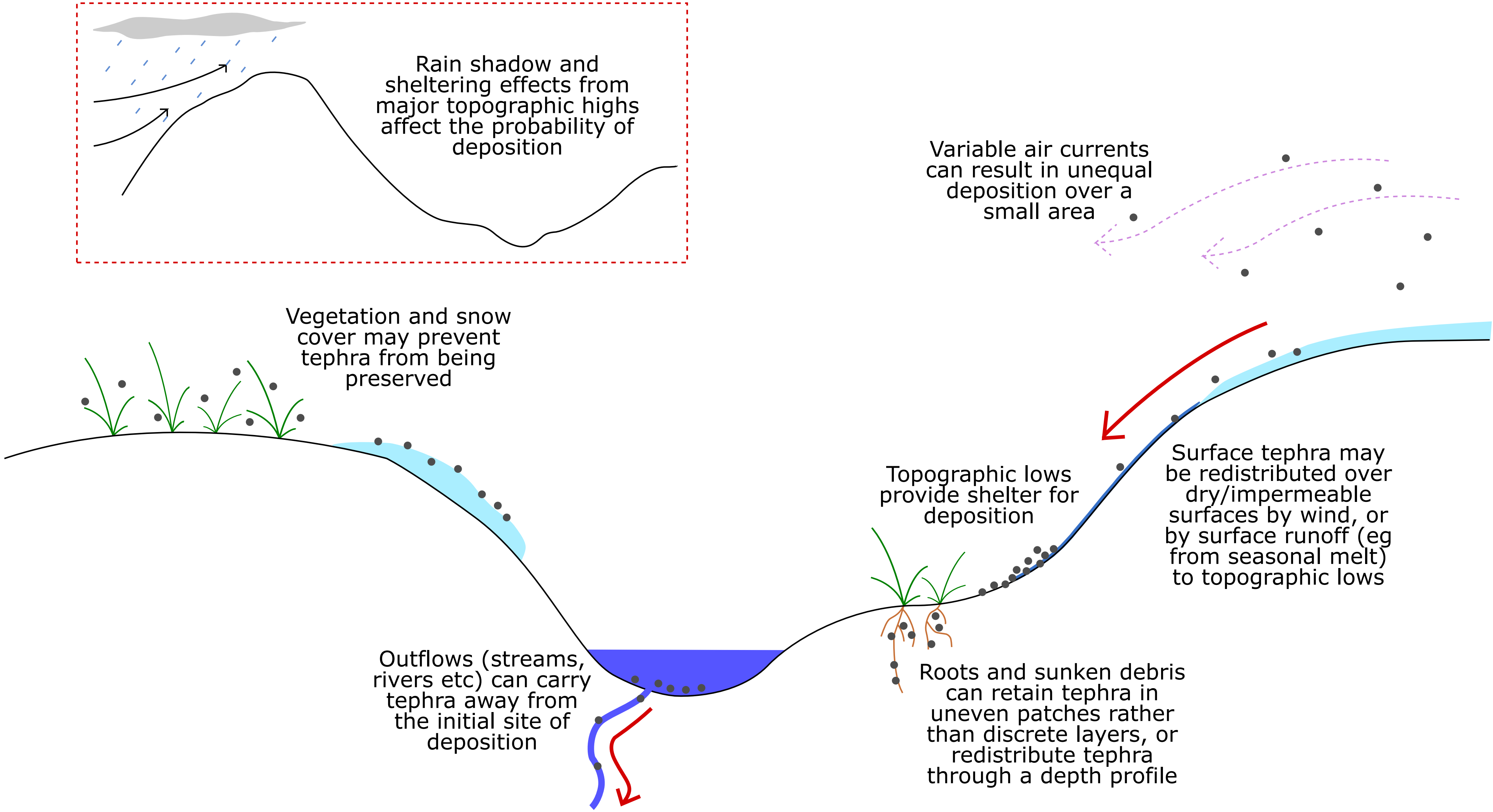

Rain shadow and sheltering effects from major topographic highs affect the probability of deposition
Variable air currents can result in unequal deposition over a small area
Vegetation and snow cover may prevent tephra from being preserved
Topographic lows provide shelter for deposition
Surface tephra may be redistributed over dry/impermeable surfaces by wind, or by surface runoff (eg from seasonal melt) to topographic lows
Outflows (streams, rivers etc) can carry tephra away from the initial site of deposition
Roots and sunken debris can retain tephra in uneven patches rather than discrete layers, or redistribute tephra through a depth profile